**ORNL/SPR-2018/959**
Rev. 0

# *Design and Thermal Analysis for Irradiation of Tensile Specimens from Wrought, Powder Metallurgy, and Additive Processed Alloys in the HFIR*

## Nuclear Technology Research and Development

***Prepared for***
***U.S. Department of Energy***
***Nuclear Technology R&D***
***Advanced Fuels Campaign***

***Annabelle G. Le Coq, Richard H. Howard,***
***Kory D. Linton, and Kevin G. Field***
***Oak Ridge National Laboratory***

***September 2018***
**M3NT-18OR020203043**

# ACKNOWLEDGMENTS

This research was sponsored by the Advanced Fuels Campaign (AFC) of the US Department of Energy (DOE), Office of Nuclear Energy. Neutron irradiation in the High Flux Isotope Reactor (HFIR) is made possible by the Office of Basic Energy Sciences, US DOE. The report was authored by UT-Battelle under Contract No. DE-AC05-00OR22725 with the US Department of Energy. Materials have been provided by David Hoelzer (Oak Ridge National Laboratory (ORNL)), Sebastien Dryepondt (ORNL), Niyanth Sridharan (ORNL), Yukinori Yamamoto (ORNL), and Stuart A. Maloy (Los Alamos National Laboratory (LANL)).

# SUMMARY

This report provides a summary of the irradiation vehicle design and thermal analysis of sub-sized tensile specimens generated through traditional processing routes (e.g. wrought alloys), powder metallurgy techniques (e.g. oxide dispersion strengthened alloys), and through additive manufacturing techniques. The neutron irradiations are planned for placement in the flux trap of the High Flux Isotope Reactor (HFIR). The irradiation vehicles are designed to have nominal target temperatures of 300°C, 385°C, or 525°C with each test train accommodating 32 sub-sized tensile specimens.

# CONTENTS

ACKNOWLEDGMENTS ........ iii

SUMMARY ........ iv

CONTENTS ........ vi

FIGURES ........ vii

TABLES ........ vii

ACRONYMS ........ ix

1. INTRODUCTION ........ 1

2. EXPERIMENTAL METHODS ........ 2
   2.1 HFIR Irradiation Experiments ........ 2
   2.2 Experiment Design Concepts ........ 2

3. COMPUTATIONAL METHODS ........ 3

4. THERMAL ANALYSIS RESULTS ........ 5
   4.1 Test Matrix ........ 5
   4.2 Temperature Contours ........ 6
   4.3 Thermal Summary ........ 10

5. SUMMARY AND CONCLUSIONS ........ 10

6. REFERENCES ........ 10

# FIGURES

Figure 1. Section view showing irradiation capsule design concept. 3

Figure 2. Core mapping for the GENTEN capsule design. 6

Figure 3. Predicted temperature contours (in °C) for a nominally 300 °C design, showing (a) the specimens, (b) the SiC temperature monitors and (c) a section view of all components. 7

Figure 4. Predicted temperature contours (in °C) for a nominally 385 °C design, showing (a) the specimens, (b) the SiC temperature monitors and (c) a section view of all components. 8

Figure 5. Predicted temperature contours (in °C) for a nominally 525 °C design, showing (a) the specimens, (b) the SiC temperature monitors and (c) a section view of all components. 9

# TABLES

Table 1. Experiment materials and material property references. 4

Table 2. Thermal boundary conditions for hydraulic tube irradiation experiments. 4

Table 3. Irradiation test matrix. 5

Table 4. Materials loading plan in the different capsules. 5

Table 5. Summary of component temperatures, irradiation position, fill gas, and cold holder-to-housing gas gap. 10

# ACRONYMS

| Acronym | Description |
|---|---|
| 3D | Three-dimensional |
| AM | Additive manufacturing |
| AMOW | Additive manufacturing, oxide dispersion strengthened, wrought |
| ATF | Accident tolerant fuel |
| CAD | Computer aided design |
| DAC | Design and analysis calculation |
| dpa | Displacements per atom |
| GENTEN | General Tensile |
| HFIR | High Flux Isotope Reactor |
| LWR | Light Water Reactor |
| NEIT | Nuclear Experiments and Irradiation Testing |
| ODS | Oxide dispersion strengthened |
| ORNL | Oak Ridge National Laboratory |
| R&D | Research & Development |
| SiC | Silicon carbide |
| TM | Temperature monitor |

# DESIGN AND THERMAL ANALYSIS FOR IRRADIATION OF TENSILE SPECIMENS FROM WROUGHT, POWDER METALLURGY, AND ADDITIVE PROCESSED ALLOYS IN THE HFIR

## 1. INTRODUCTION

A range of Fe-based alloys using various compositions and processing techniques are currently being considered for both accident tolerant fuel (ATF) applications in currently operating commercial light water reactors (LWRs) and for advanced reactor applications. Both applications require materials which can perform under extreme environments including elevated temperatures, high displacement damage (>10 displacements per atom (dpa)), and corrosive conditions. Unique metallurgical controls are used to optimize material performance in these extreme environments. As an example, C26M [1] is a wrought FeCrAl alloy being developed for ATF cladding that uses a balance of the major alloying elements (Cr, Al, and Fe) to achieve the necessary high temperature oxidation for accident tolerance while still maintaining low enough levels of Cr and Al to provide enhanced radiation tolerance and allow for processing of thin walled tubes. Another group of alloys that are being developed use powder metallurgy processing techniques to form nano-clusters/nano-oxides within the microstructure to improve radiation tolerance and elevated temperature (>500°C) creep strength. This group of alloys are referred to as oxide dispersion strengthened (ODS) alloys. These alloys – 14YWT [2, 3], 9YWTV [4], OFRAC [5], 106ZYA15C, and 106ZY10C [6] – also use compositional control to tailor the nanofeatures present in the as-processed condition as well as promote elevated temperature corrosion and oxidation resources. Another group of alloys – HT9 [7], 300SS-ODS, and Grade 91 (Gr91) [8] – use additive manufacturing (AM) techniques to enable unique microstructures and complex shapes/geometries that can only be achieved using the unique time-temperature consolidation profiles possible using additive techniques. These three material classes – wrought, ODS, and AM – cover a wide range of novel alloys that could have a large impact on nuclear energy systems. However, significant research and development (R&D) of these alloys is required before these materials can be deployed.

The R&D programs for these wrought, ODS, and AM alloys are still in their infancy. As such, there is very limited data on the broad range of material properties required for commercial deployment. One of the most significant gaps in the material performance database for these alloys is the performance of the alloys within an elevated temperature (>275°C) neutron radiation environment. More specifically, the performance of these alloys as a function of both irradiation dose and irradiation temperature are lacking. To fill these gaps, an irradiation campaign was conceived and developed to quickly generate both mechanical property and microstructural evolution data. This campaign was deemed the **A**dditive **M**anufacturing, **O**xide Dispersion Strengthened, **W**rought (AMOW) irradiation campaign.

The AMOW irradiation campaign targets neutron irradiations in the High Flux Isotope Reactor (HFIR) at Oak Ridge National Laboratory (ORNL) due to the HFIR’s ability to generate high damage doses (~8-12 dpa per calendar year in pure Fe), allowing for rapid screening of radiation tolerance. The AMOW campaign also leverages previous irradiation campaigns and irradiation vehicle design concepts including the FCAY [9] and FCAT campaigns [10]. The AMOW campaign is structured to capture at least three irradiations doses (nominally 8, 16, and 50 dpa) at three separate temperatures: 300°C, 385°C, and 525°C. The irradiation temperatures are selected to simulate common irradiation temperatures for both LWRs and several advanced reactor concepts while the doses represent low, moderate, and high damage doses for many reactor concepts. The SS-J2 [11] tensile specimen geometry was selected for use in the irradiation campaign because mechanical performance (e.g. strength and ductility parameters) has historically shown good comparison with that of larger standard-sized tensile specimens while minimizing the total specimen volume. This report summarizes the AMOW irradiation campaign including the determined irradiation conditions and the methods to derive them.

# 2. EXPERIMENTAL METHODS

## 2.1 HFIR Irradiation Experiments

The irradiation experiments described in this document will be performed in the flux trap of ORNL's HFIR. The HFIR is a beryllium-reflected, pressurized, light water–cooled and moderated flux trap–type reactor [12]. The core consists of aluminum-clad involute-fuel plates which currently use highly enriched $^{235}U$ fuel at a power level of 85 MW. A typical HFIR cycle is 25 days. The reactor core consists of two concentric annular regions, each approximately 61 cm in height. The flux trap region is located inside the fuel region. The HFIR fuel and all experiment vessels are cooled by the reactor's primary coolant, which is approximately 50–60°C.

The goal of this work is to design experiments to contain the tensile specimens inside HFIR-approved irradiation vehicles so that they can accumulate the desired dose while being irradiated at the design temperature. Neutron and gamma radiation from the HFIR fuel cause heating of the experiment test coupons which are contained within the irradiation vehicles. This heating is accurately determined using neutronics models of the HFIR core. The data from the neutronics models are then used as inputs for thermal analyses to predict component temperatures during irradiation. Experiments in the flux trap are almost always un-instrumented; passive silicon carbide (SiC) temperature monitors (TMs) can be used to determine the irradiation temperature post-irradiation [13]. However, detailed neutronic and thermal analyses are required to ensure that design temperatures are achieved. Experiment designs typically use a small insulating gas gap to achieve the desired specimen temperature(s). The size of the gap and the choice of the fill gas (typically helium (He), neon (Ne), or argon (Ar)) inside the experiment are established so that the heat generated in the experimental components passes through the gas gap and results in the desired temperature drop across the gap. The temperature drop is a function of the heat flux through the gap, the thermal conductivity of the fill gas, and the size of the gas gap. Similar analyses have been performed for previous HFIR experiments [14-18].

## 2.2 Experiment Design Concepts

The overall design of the irradiation experiments developed in this work is shown in the section view of Figure 1. The outer containment for the irradiation experiment is the capsule housing (known as a "rabbit"), which is directly cooled on the outer surface by the HFIR's primary coolant. This flexible design, referred to as the **GEN**eral **TEN**sile (GENTEN) capsule design consists of three specimen holders stacked axially within the rabbit containment. These three holder assemblies, each with a square cutout, are inserted into the housing. Holders are made of either aluminum (generally for lower temperatures, 200°C-375°C) or molybdenum (for higher temperatures, 375°C-1200°C). Each holder assembly contains four sets of three 0.5-mm thick tensile specimens and a passive SiC TM, which is located adjacent to the innermost specimen. A spring pin is placed in the center of each holder to press the stacked specimens against the holder walls. Chevrons are placed on either side of the tensile specimen gage sections to ensure uniform heat generation within the holder and adequate heat rejection from the specimen gauge sections. In this way, each set of three specimens and two chevrons closely resembles a single 1.5 mm × 4.0 mm × 16.0 mm solid parallelepiped coupon. Temperature is controlled by varying the concentration of a He/Ar gas mixture and the size of the gas gap between the holders and the housing. Varying the gas mixture changes the effective thermal conductivity of the gas gap. Tabs located on the outside of the holders keep the holders radially centered inside the housing. This minimizes azimuthal variations in the gas gaps between the holders and the housing. Stainless steel wave springs at the top and the bottom of the capsule keep the holders axially centered and reduce axial heat loss from the holders to the housing. Grafoil foil spacers are also stacked on the bottom end of the capsule to further reduce axial heat losses.

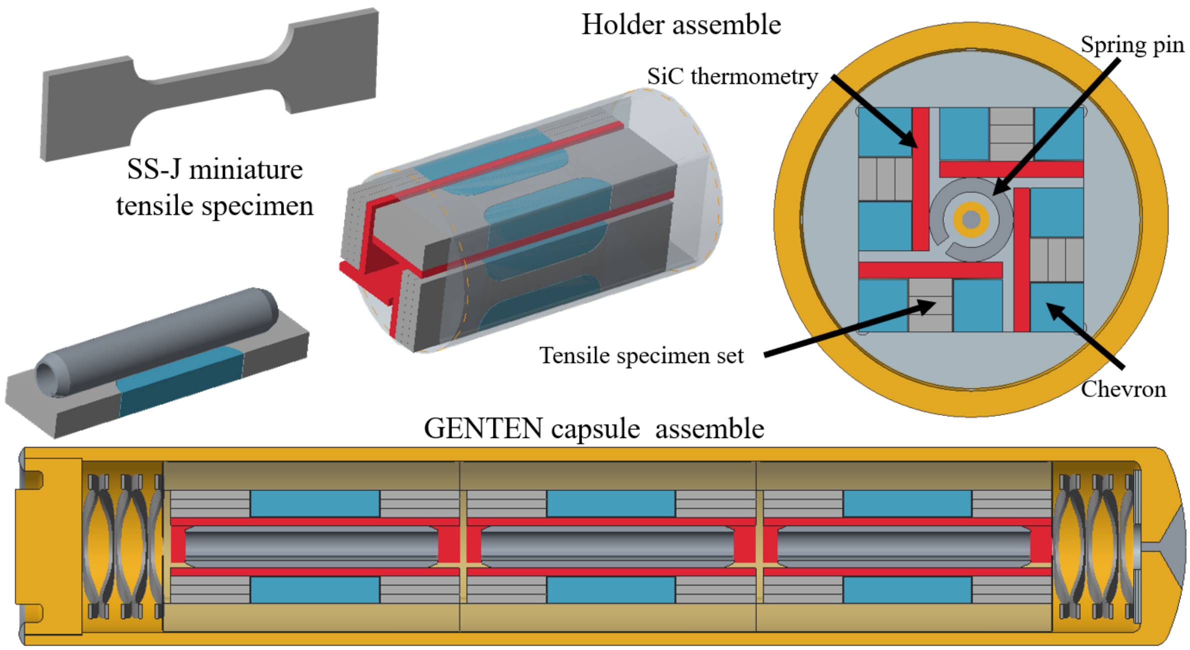


**Figure 1. Section view showing irradiation capsule design concept.**

## 3. COMPUTATIONAL METHODS

Three-dimensional (3D) thermal analyses are performed using the ANSYS finite element software package to predict temperature distributions inside the experiment. These analyses use material-dependent heat generation rates (heat per unit mass) calculated from neutronics analyses. Custom user-defined macros have been incorporated into ANSYS to determine thermal contact conductance between components either in contact or separated by small gas gaps that expand or contract due to thermal expansion [19]. In this way, gas gaps are not directly meshed, which significantly reduces computational time. Computer aided design (CAD) models are imported into ANSYS and meshed with a mesh size ranging from 0.2–0.7 mm. Thermal contacts are defined to allow heat to be transferred between multiple bodies. Gas gap heat transfer is assumed to only result from conduction and radiation, as there is very little space available for natural convection to occur. Gaps are typically on the order of tens of microns to hundreds of microns, and the total internal length of the capsule is less than 60 mm. The solution methods accounts for thermal expansion using temperature-dependent thermal expansion data, the temperatures of contact, and target surface nodes.

The ORNL Nuclear Experiments and Irradiation Testing (NEIT) group maintains a database of design and analysis calculations (DACs) that include temperature-dependent thermophysical material properties used in thermal analyses. Some properties for SiC also include radiation dose-dependence. Properties are primarily obtained from CINDAS [20], MatWeb [21], and various literature sources. Properties of gas mixtures are calculated using the methods described by Wahid et al. [22]. Material properties for this calculation are included in the DACs, as shown in Table 1 and are available upon request.

**Table 1. Experiment materials and material property references.**

| Part | Material | Reference |
|---|---|---|
| Housing, end cap, and holders | Aluminum | DAC-10-03-PROP_AL6061 [23] |
| Specimens and chevrons | FeCrAl | DAC-16-02-PROP_FeCrAl [24] |
| Specimens and chevrons | F82H | DAC-10-10-PROP_F82H [25] |
| Springs, spring pins, and chevrons | 304 SS | DAC-10-16-PROP_SS304 [26] |
| Holders | Molybdenum | DAC-10-11-PROP_MOLY [27] |
| Foil spacers | Grafoil | DAC-11-16-PROP_GRAFOIL [28] |
| TMs | SiC | DAC-10-06-PROP_SIC(IRR) [29] |
| Fill gas | Argon | DAC-10-09-PROP_ARGON [30] |
| Fill gas | Helium | DAC-10-02-PROP_HELIUM [31] |

Convection boundary conditions are applied to the outer surface of the housing. Details of the calculation of the convective heat transfer coefficients and bulk coolant temperatures are summarized in DAC-11-01-RAB03 [32]. These parameters were calculated using turbulent flow correlations and the axial power profile (resulting from neutron and gamma heat generation in the coolant) specific to the hydraulic tube facility in the HFIR flux trap. Temperatures calculated in the thermal analyses are not extremely sensitive to the convection heat transfer coefficient, as the housing surface temperatures are typically only ~10°C warmer than the bulk coolant temperature.

The heat generation rates vary as a function of axial position from the midplane of the flux trap region in the reactor core. Peak heat generation rates (at the core midplane), parameters for determining the axial profile, and convection parameters are summarized in Table 2. The correlation parameter was determined in DAC-10-18-RAB02 [33] and all heat generation rate were calculated in C-HFIR-2012-035 [34]. These heat generation rates include contributions from prompt neutrons, fission photons, and secondary photons produced by the fission neutrons, fission product decay photons, and decay (primarily due to beta emission) of activation sources. Nuclear heating in the HFIR is dominated by photon absorption in the materials used in this experiment.

**Table 2. Thermal boundary conditions for hydraulic tube irradiation experiments.**

| Parameter | | Value |
|---|---|---|
| Heat transfer coefficient | $h_c$ | 47.1 kW m$^{-2}$ K$^{-1}$ |
| Bulk coolant temperature | $T_{bulk}$ | 52°C |
| Correlating parameter | $(\sigma)$ | 30.07 cm |
| Peak heat generation rate for aluminum | $q_{peak}(Al)$ | 31.3 W/g |
| Peak heat generation rate for steels | $q_{peak}(St)$ | 38.1 W/g |
| Peak heat generation rate for molybdenum | $q_{peak}(Mo)$ | 42.0 W/g |
| Peak heat generation rate for grafoil | $q_{peak}(C)$ | 32.5 W/g |
| Peak heat generation rate for SiC | $q_{peak}(SiC)$ | 31.7 W/g |

The local heat generation rate is estimated using the following profile:

$$q(\text{material}, z) = q_{\text{peak}}(\text{material}) \cdot \exp\left[-\left(\frac{z}{\sigma}\right)^2\right],$$

where:

q = local heat generation rate as a function of the material and axial location,
z = axial location in the HFIR, where the midplane is at z = 0, and

# 4. THERMAL ANALYSIS RESULTS

## 4.1 Test Matrix

Table 3 summarizes the irradiation conditions for the different capsules. Eleven capsules, each containing 32 tensile specimens, will be irradiated. Three material types will be studied: wrought materials, ODS alloys, and AM alloys. For each specimen type, a number of specimens will be tested with slight variations in chemical composition, heat treatment, or fabrication orientation. Table 4 shows the number of specimens of each material that are planned to be loaded in each capsule.

**Table 3. Irradiation test matrix.**

| Capsule number | Irradiation temperature | Irradiation dose (dpa) | Material type |
|---|---|---|---|
| Capsule #1 | 300 °C | 8 | Wrought<br>ODS<br>AM |
| Capsule #2 | | 16 | |
| Capsule #3 | | 50 | |
| Capsule #4 | 385 °C | 8 | |
| Capsule #5 | | 16 | |
| Capsule #6 | | 50 | |
| Capsule #7 | | 76 | |
| Capsule #8 | 525 °C | 8 | |
| Capsule #9 | | 16 | |
| Capsule #10 | | 50 | |
| Capsule #11 | | 76 | |

**Table 4. Materials loading plan in the different capsules.**

| Material type | Base alloy | ID* | Number of specimens per capsule | | | | | | | | | | |
|---|---|---|---|---|---|---|---|---|---|---|---|---|---|
| | | | #1 | #2 | #3 | #4 | #5 | #6 | #7 | #8 | #9 | #10 | #11 |
| Wrought | C26M | CW*XX* | 2 | 2 | 2 | 3 | 3 | 3 | 3 | 3 | 3 | 3 | 3 |
| | | CH*XX* | 2 | 2 | 2 | 3 | 3 | 3 | 3 | 3 | 3 | 3 | 3 |
| ODS | 14YWT | YW*XX* | 2 | 2 | 3 | 3 | 4 | 4 | 3 | 3 | 4 | 4 | 4 |
| | 9YWTV | 9Y*XX* | 2 | 2 | 2 | 3 | 4 | 4 | 3 | 3 | 4 | 4 | 4 |
| | OFRAC | OF*XX* | 2 | 2 | 3 | 3 | 4 | 4 | 3 | 3 | 4 | 4 | 4 |
| | 106ZYA15C | FO*XX* | 2 | 2 | 2 | 3 | 3 | 3 | 3 | 3 | 3 | 3 | 3 |
| | 106ZY10C | FC*XX* | 2 | 2 | 2 | 3 | 3 | 3 | 3 | 3 | 3 | 3 | 3 |
| AM | HT9 | XA*XX* | 2 | 2 | 2 | 1 | | | 1 | 1 | | | |
| | | ZA*XX* | 2 | 2 | 2 | 1 | | | 1 | 1 | | | |
| | | XB*XX* | 2 | 2 | 2 | 1 | | | 1 | 1 | | | |
| | | YB*XX* | 2 | 2 | 2 | 1 | | | 1 | 1 | | | |
| | | XF*XX* | 2 | 2 | 2 | 1 | | | 1 | 1 | | | |
| | | ZF*XX* | 2 | 2 | 2 | 1 | | | 1 | 1 | | | |
| | | HL*XX* | 2 | 2 | 2 | 3 | 2 | 2 | 3 | 3 | 2 | 2 | 2 |
| | | HN*XX* | 2 | 2 | 2 | 2 | 2 | 2 | 2 | 2 | 2 | 2 | 2 |
| | 300SS-ODS | SX*XX* | 1 | 1 | 1 | 1 | 2 | 2 | 1 | 1 | 2 | 2 | 2 |
| | | SZ*XX* | 1 | 1 | 1 | 1 | 2 | 2 | 1 | 1 | 2 | 2 | 2 |
| | | 3X*XX* | 1 | 1 | 1 | 1 | 2 | 2 | 1 | 1 | 2 | 2 | 2 |
| | | 3Z*XX* | 1 | 1 | 1 | 1 | 2 | 2 | 1 | 1 | 2 | 2 | 2 |
| | T91 | XT*XX* | 1 | 1 | | | | | | | | | |
| | | ZT*XX* | 1 | 1 | | | | | | | | | |

**XX*: ID number (01, 02, 03, …)

## 4.2 Temperature Contours

As stated earlier, the NEIT group has established the GENTEN design to be flexible for a wide range of temperatures and HFIR irradiation facility positions. This full mapping of the core (see Figure 2) allows for specific capsule configurations to be picked from a table of data, based on other parameters such as target temperature and HFIR core availability. The legend indicates XX-YY-TRRHN, where XX is the holder material, YY the fill gas, and N the axial position of the capsule numbered from bottom (1) to top (7), with position 4 located at the vertical midplane of the core. TRRH refers to target rod rabbit holders, which hold the capsules during irradiation. The red data set refers to capsules with aluminum holders and 100% helium fill gas. The green data set refers to capsules with molybdenum holders and 100% helium fill gas. The blue data set refers to capsules with molybdenum holders and a 60% helium fill gas (argon balance), which is a neon equivalent mixture. The effective temperature span of the design is 150°C-1200°C.

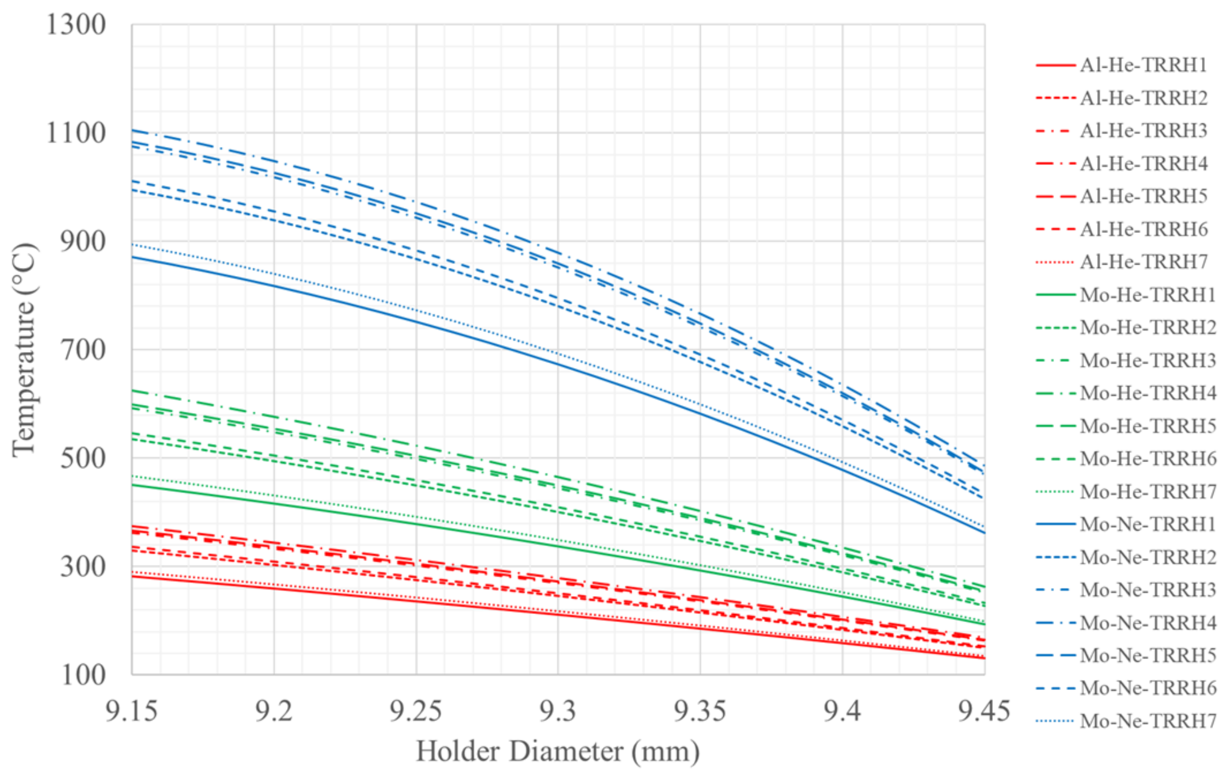


**Figure 2. Core mapping for the GENTEN capsule design.**

Figure 3, Figure 4, and Figure 5 show temperature contours (in °C) predicted by the thermal analyses, for the 300°C, 385°C and 525°C designs, respectively. The temperatures remain within ± 10% from the design temperature across the specimens, with an even tighter span across the gage lengths of the specimens.

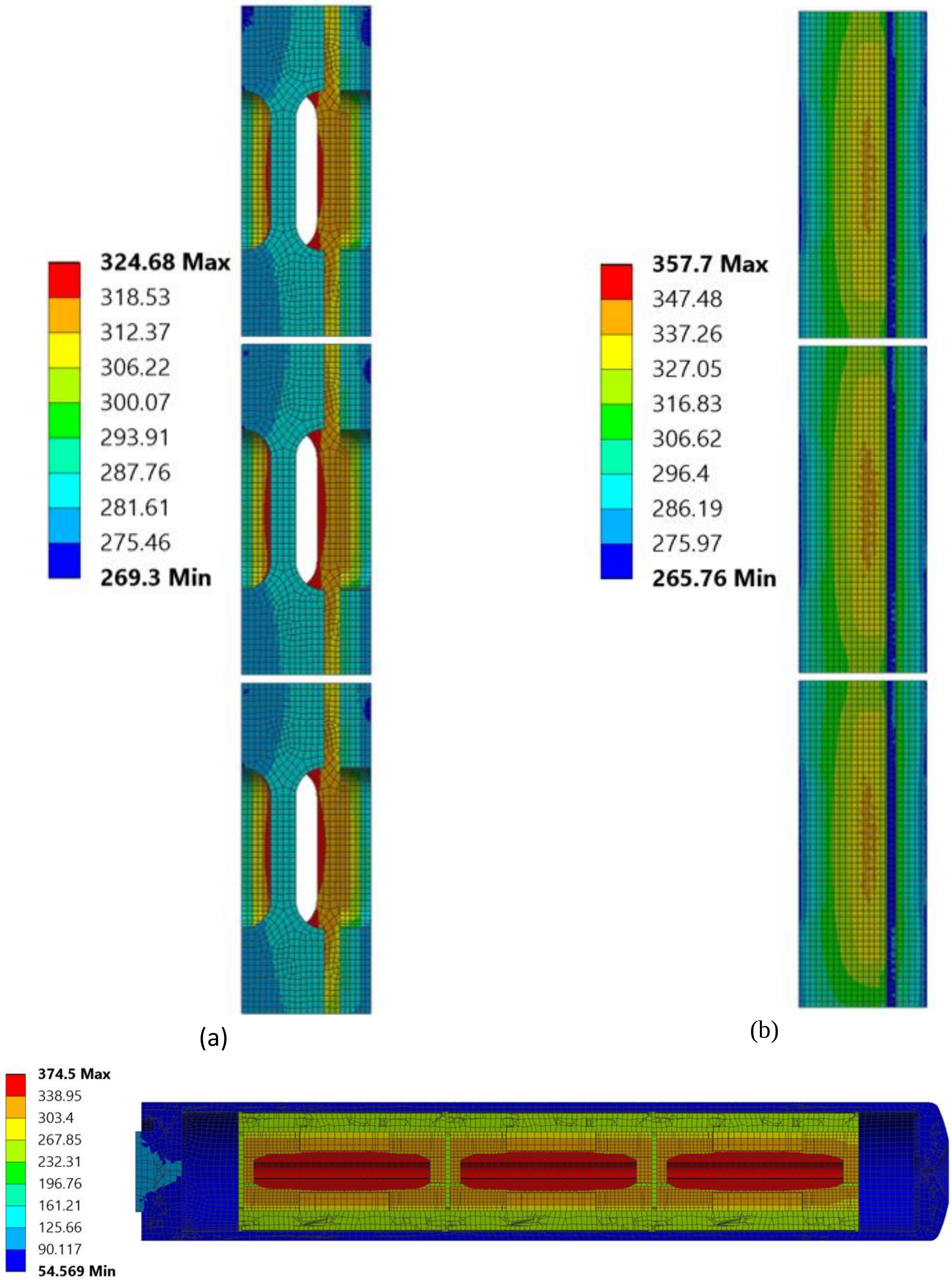


(a) (b)

(c)

**Figure 3. Predicted temperature contours (in °C) for a nominally 300 °C design, showing (a) the specimens, (b) the SiC temperature monitors and (c) a section view of all components.**

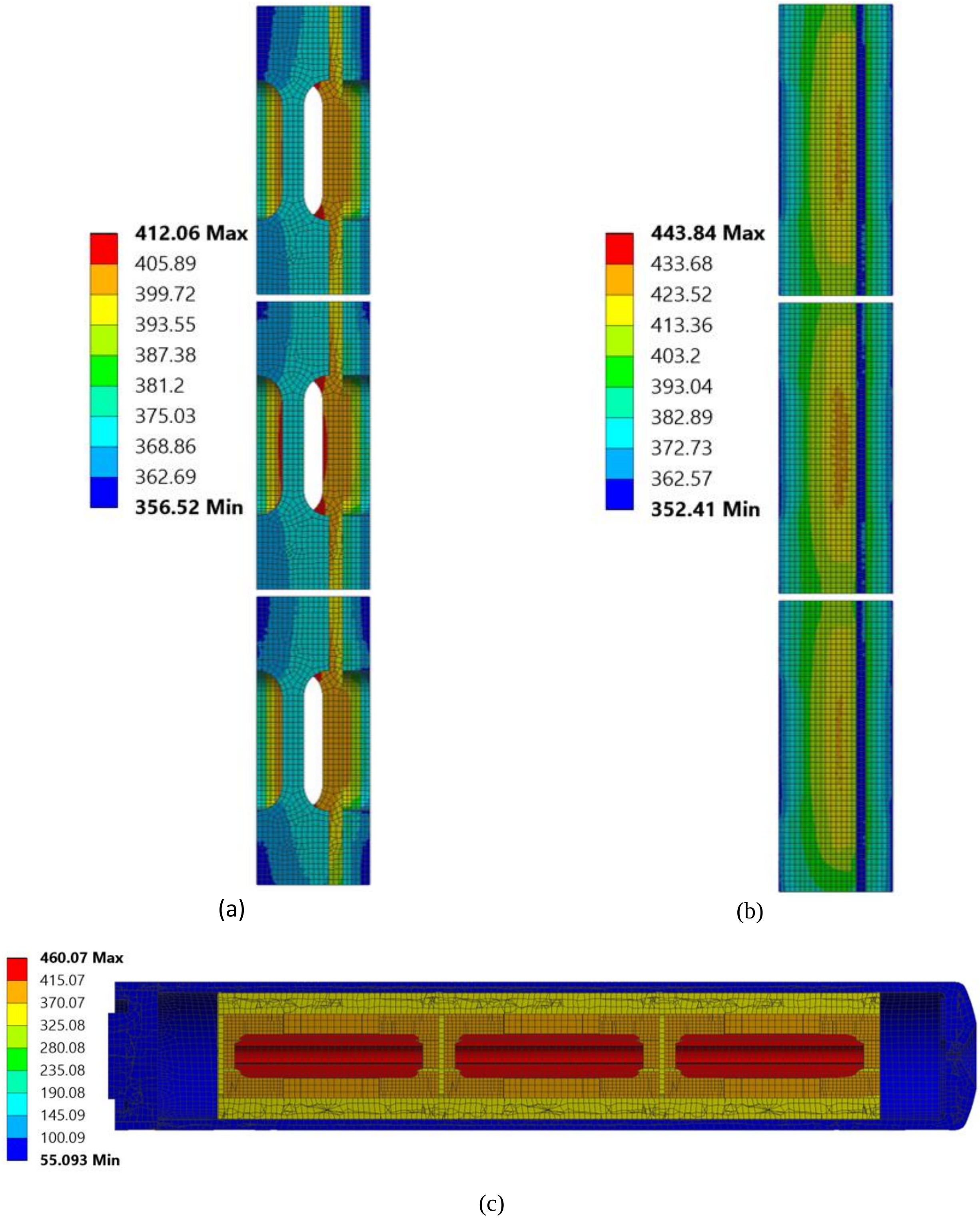


**Figure 4. Predicted temperature contours (in °C) for a nominally 385 °C design, showing (a) the specimens, (b) the SiC temperature monitors and (c) a section view of all components.**

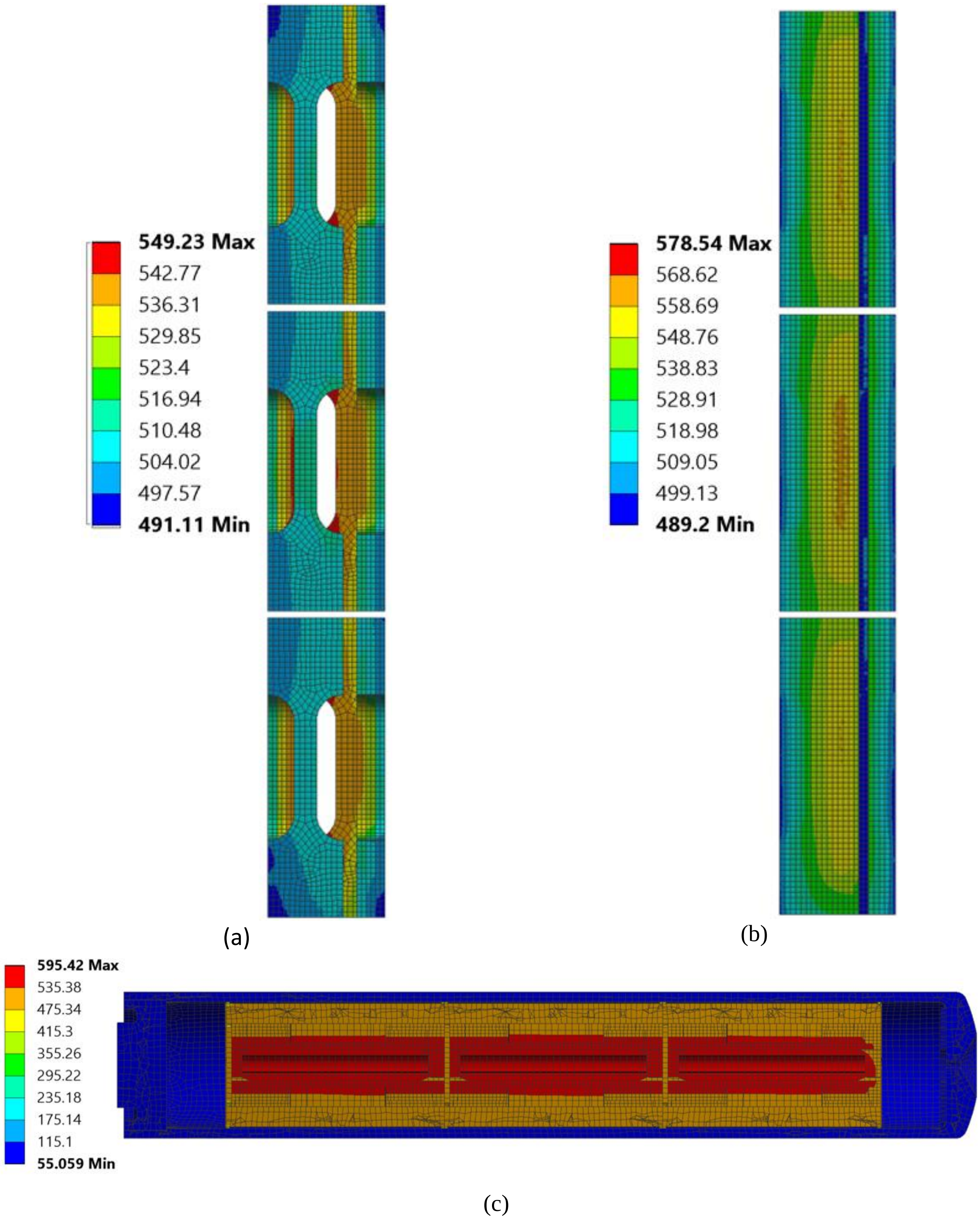


**Figure 5. Predicted temperature contours (in °C) for a nominally 525 °C design, showing (a) the specimens, (b) the SiC temperature monitors and (c) a section view of all components.**

## 4.3 Thermal Summary

Table 5 summarizes average, minimum, and maximum temperatures for the specimens, TMs, and the capsule housing, in addition to other design parameters such as the irradiation position, gas gap, and fill gas. Note that these reported values represent the cases shown in Section 4.2, and results vary somewhat, based on the flux trap axial irradiation position that is selected. This is primarily driven by the axial power profile of the HFIR, which has a steeper gradient on the peripheral positions.

**Table 5. Summary of component temperatures, irradiation position, fill gas, and cold holder-to-housing gas gap.**

| Flux trap axial position | Fill gas | Gas gap | Part | Temperature (°C) | | |
|---|---|---|---|---|---|---|
| | | | | Average | Minimum | Maximum |
| **300°C design (Al holder)** | | | | | | |
| 4 | He | 124 µm | Specimen | 301 | 269 | 324 |
| | | | TM | 317 | 256 | 358 |
| | | | Housing | 60 | 55 | 65 |
| **385°C design (Mo holder)** | | | | | | |
| 4 | He | 74 µm | Specimen | 387 | 357 | 412 |
| | | | TM | 403 | 352 | 444 |
| | | | Housing | 65 | 55 | 71 |
| **525°C design (Mo holder)** | | | | | | |
| 4 | He | 134 µm | Specimen | 524 | 491 | 549 |
| | | | TM | 539 | 482 | 579 |
| | | | Housing | 65 | 55 | 72 |

# 5. SUMMARY AND CONCLUSIONS

This report summarizes the capsule design and thermal analysis that was performed for irradiation testing of tensile specimens from wrought materials, ODS alloys, and AM alloys in the HFIR. The rabbit capsule design allows for 32 tensile specimens to be loaded. Temperature is controlled by varying the backfill gas (He or He/Ar mixture). The next step for this work is to order and inspect the different capsule components, for an expected start of capsules assembly by the end of calendar year 2018. The testing results of this campaign will help develop new alloys with high performance for use in current LWRs as well as in advanced reactor designs.

# 6. REFERENCES

1. Y. Yamamoto, Z. Sun, *Quality optimization of commercial FeCrAl tube production*, ORNL/TM-2017/338, 2017.
2. D.T. Hoelzer, *History and Outlook of ODS/NFA Ferritic Alloys for Nuclear Applications*,, Trans. Am. Nucl. Society, 2018. http://ansannual.org/wp-content/2018/Data/pdfs/626-25239.pdf (accessed August 10, 2018).

3. D.T. Hoelzer, K.A. Unocic, M.A. Sokolov, T.S. Byun, *Influence of processing on the microstructure and mechanical properties of 14YWT*, J. Nucl. Mater., 2016, **471**: p. 251–265, DOI: 10.1016/J.JNUCMAT.2015.12.011.
4. T.S. Byun, J.H. Yoon, D.T. Hoelzer, Y.B. Lee, S.H. Kang, S.A. Maloy, *Process development for 9Cr nanostructured ferritic alloy (NFA) with high fracture toughness*, J. Nucl. Mater. , 2014, **449**: p. 290–299, DOI: 10.1016/J.JNUCMAT.2013.10.007.
5. C.P. Massey, D.T. Hoelzer, P.D. Edmondson, R.L. Seibert, A. Kini, B. Gault, K.A. Terrani, S.J. Zinkle, *OFRAC: An Advanced Nanostructured Ferritic Alloy Fuel Cladding for Fast Reactors*, 2018. http://ansannual.org/wp-content/2018/Data/pdfs/572-25124.pdf (accessed August 10, 2018).
6. S.N. Dryepondt, C.P. Massey, P.D. Edmondson, *2nd Gen FeCrAl ODS Alloy Development For Accident-Tolerant Fuel Cladding*, ORNL/TM-2016/456, 2016. DOI: 10.2172/1362225.
7. N. Sridharan, K.G. Field, *Preliminary Characterization and Mechanical Performance of Additively Manufactured HT9*, ORNL/SPR-2018/780, 2018.
8. T.J. Maloy, S. Andrew, *Laser Additive Manufacturing of F/M Steels for Radiation Tolerant Nuclear Components Intended for*, LA-UR-17-30052, 2017. https://permalink.lanl.gov/object/tr?what=info:lanl-repo/lareport/LA-UR-17-30052 (accessed August 10, 2018).
9. K.G. Field, S.A. Briggs, P.D. Edmondson, J.C. Haley, R.H. Howard, X. Hu, K.C. Littrell, C.M. Parish, Y. Yamamoto, *Database on Performance of Neutron Irradiated FeCrAl Alloys*, ORNL/TM-2016/335, 2016.
10. K.G. Field, Y. Yamamoto, R.H. Howard, *Status of Post Irradiation Examination of FCAB and FCAT Irradiation Capsules*, ORNL/TM-2016/558, 2016.
11. M.N. Gussev, R.H. Howard, K.A. Terrani, K.G. Field, *Sub-size tensile specimen design for in-reactor irradiation and post-irradiation testing*, Nucl. Eng. Des. , 2017, **320**: p. 298-308, DOI: 10.1016/j.nucengdes.2017.06.008.
12. *High Flux Isotope Reactor Technical Parameters*. Available from: http://neutrons.ornl.gov/hfir/parameters.
13. A. Campbell, et al., *Method for analyzing passive silicon carbide thermometry with a continuous dilatometer to determine irradiation temperature*, Nuclear Instruments and Methods in Physics Research B, 2016, **370**: p. 49–58.
14. Christian M. Petrie, et al., *Experimental design and analysis for irradiation of SiC/SiC composite tubes under a prototypic high heat flux*, Journal of Nuclear Materials, 2017, **491**: p. 94–104, DOI: https://doi.org/10.1016/j.jnucmat.2017.04.058.
15. Christian M. Petrie, Kurt R. Smith, and Tyler J. Gerczak, *Design and Thermal Analysis for Irradiation of Pyrolytic Carbon/Silicon Carbide Diffusion Couples in the High Flux Isotope Reactor*, ORNL/TM-2017/390, Oak Ridge National Lab, Oak Ridge, TN, 2017. https://www.osti.gov/servlets/purl/1399950.
16. Christian M. Petrie, et al., *Analysis and Experimental Qualification of an Irradiation Capsule Design for Testing Pressurized Water Reactor Fuel Cladding in the High Flux Isotope Reactor*, ORNL/TM-2017/67, Oak Ridge National Laboratory, Oak Ridge, TN, 2017.
17. Richard H. Howard and Kurt R. Smith, *Development of a Flexible Design for Irradiation of Miniature Tensile and Charpy Test Specimens in the High Flux Isotope Reactor*, ORNL/TM-2018/872, Oak Ridge National Lab, Oak Ridge, TN, 2018. https://www.osti.gov/servlets/purl/1460197.
18. C.M. Petrie and T. Koyanagi, *Assembly and Delivery of Rabbit Capsules for Irradiation of Silicon Carbide Cladding Tube Specimens in the High Flux Isotope Reactor*, ORNL/TM-2017/433, Oak Ridge National Laboratory, Oak Ridge, TN, 2017.

19. J.L. McDuffee. *Heat Transfer Through Small Moveable Gas Gaps in a Multi-Body System Using the ANSYS Finite Element Software*. in *ASME 2013 Heat Transfer Summer Conference*. 2013. Minneapolis, MN.
20. LLC CINDAS, *Global Benchmark for Critically Evaluated Materials Properties Data*. cited 27 July, 2016.
21. MatWeb. *Material Property Data*. [cited 2016 July 27]; Available from: http://matweb.com/.
22. S.M.S Wahid and C.V. Madhusudana, *Gap conductance in contact heat transfer*, International Journal of Heat and Mass Transfer, 2000, **43**: p. 4483–4487.
23. J.L. McDuffee, *Thermophysical Properties for AL6061*, DAC-10-03-PROP_AL6061, Rev.2,, Oak Ridge National Laboratory, Thermal Hydraulics and Irradiation Engineering Group, Oak Ridge, TN, 2013.
24. C.M. Petrie, *Thermophysical Properties for FeCrAl*, DAC-16-02-PROP_FeCrAl, Rev.0, Oak Ridge National Laboratory, Oak Ridge, TN,, 2016.
25. R.H. Howard, *Thermophysical Properties for F82H Steel*, DAC-10-10-PROP_F82H, Rev.1, Oak Ridge National Laboratory, Oak Ridge, TN, 2016.
26. J.L. McDuffee, *Thermophysical Properties for 304 Stainless Steel*, DAC-10-16-PROP_SS304, Rev.1, Oak Ridge National Laboratory, Oak Ridge, TN, 2013.
27. J.L. McDuffee, *Thermophysical Properties for Molybdenum*, DAC-10-11-PROP_MOLY, Rev. 1, Oak Ridge National Laboratory, Oak Ridge, TN, 2013.
28. J.L. McDuffee, *Thermophysical Properties for Flexible Graphite*, DAC-11-16-PROP_GRAFOIL, Rev. 0,, Oak Ridge National Laboratory, Oak Ridge, TN, 2013.
29. J.L. McDuffee, *Thermophysical Properties for Irradiated SiC*, DAC-10-06-PROP_SIC(IRR), Rev. 2, Oak Ridge National Laboratory, Thermal Hydraulics and Irradiation Engineering Group, Oak Ridge, TN, 2013.
30. J.L. McDuffee, *Thermophysical Properties for Argon*, DAC-10-09-PROP_ARGON, Rev. 0, Oak Ridge National Laboratory, Thermal Hydraulics and Irradiation Engineering Group, Oak Ridge, TN, 2010.
31. J.L. McDuffee, *Thermophysical Properties for Helium*, DAC-10-02-PROP_HELIUM, Rev. 0, Oak Ridge National Laboratory, Thermal Hydraulics and Irradiation Engineering Group, Oak Ridge, TN, 2010.
32. J.L. McDuffee, *Heat Transfer Coefficients and Bulk Temperatures for HFIR Rabbit Facilities*, DAC-11-01-RAB03, Rev. 0, Oak Ridge National Laboratory, Thermal Hydraulics and Irradiation Engineering Group, Oak Ridge, TN, 2011.
33. J.L. McDuffee, *Heat Generation Rates for Various Rabbit Materials in the Flux Trap of HFIR*, DAC-10-18-RAB02, Rev. 0, Oak Ridge National Laboratory, Thermal Hydraulics and Irradiation Engineering Group, Oak Ridge, TN, 2011.
34. J L McDuffee, *Heat Generation Rates for Various Rabbit Materials in the Flux Trap of HFIR*, C-HFIR-2012-035, Rev. 0 Oak Ridge National Laboratory, Oak Ridge, TN, 2012.